
This is an electronic reprint of the original article.
This reprint may differ from the original in pagination and typographic detail.

Esfandiari, Majdoddin; Vorobyov, Sergiy A.; Heath, Robert W.

Sparsity Enforcing with Toeplitz Matrix Reconstruction Method for Mmwave UI Channel Estimation with One-Bit Adcs

Published in:
2022 IEEE 12th Sensor Array and Multichannel Signal Processing Workshop, SAM 2022

DOI:
[10.1109/SAM53842.2022.9827806](https://doi.org/10.1109/SAM53842.2022.9827806)

Published: 01/01/2022

Document Version
Peer-reviewed accepted author manuscript, also known as Final accepted manuscript or Post-print

Please cite the original version:
Esfandiari, M., Vorobyov, S. A., & Heath, R. W. (2022). Sparsity Enforcing with Toeplitz Matrix Reconstruction Method for Mmwave UI Channel Estimation with One-Bit Adcs. In *2022 IEEE 12th Sensor Array and Multichannel Signal Processing Workshop, SAM 2022* (pp. 141-145). (Proceedings of the IEEE Sensor Array and Multichannel Signal Processing Workshop). IEEE. <https://doi.org/10.1109/SAM53842.2022.9827806>

This material is protected by copyright and other intellectual property rights, and duplication or sale of all or part of any of the repository collections is not permitted, except that material may be duplicated by you for your research use or educational purposes in electronic or print form. You must obtain permission for any other use. Electronic or print copies may not be offered, whether for sale or otherwise to anyone who is not an authorised user.

SPARSITY ENFORCING WITH TOEPLITZ MATRIX RECONSTRUCTION METHOD FOR MMWAVE UL CHANNEL ESTIMATION WITH ONE-BIT ADCS

Majdoddin Esfandiari*, Sergiy A. Vorobyov*, and Robert W. Heath Jr.†

*Department of Signal Processing and Acoustics, Aalto University, Espoo, Finland

†Department of Electrical and Computer Engineering, North Carolina State University, Raleigh, USA

ABSTRACT

One-bit analog-to-digital converters enable digital beamforming in millimeter wave (mmWave) multi-input multi-output communication systems with low power consumption. Conventional signal processing tasks like channel estimation, though, are challenging due to the extreme quantization, making it challenging to implement uplink (UL) multiuser receivers. We reformulate the UL channel estimation problem as a multiplication of two specific matrices, and then we leverage Toeplitz matrix reconstruction in conjunction with the angular domain sparsity of the UL channel to recover UL channel via solving a properly designed optimization problem. Our new approach is called the sparsity enforcing with Toeplitz matrix reconstruction (SE-TMR) method. Numerical simulations are carried out to showcase the advantages of SE-TMR over existing competitive methods in terms of normalized mean squared error in clustered narrowband channels.

Index Terms— Multi-user MIMO, uplink channel estimation, one-bit analog-to-digital converter, angular domain, Toeplitz matrix reconstruction.

1. INTRODUCTION

Millimeter-wave (mmWave) multiple-input multiple-output (MIMO) communications is an approach that extends the high data rate benefits associated with the use of mmWave to take advantage of multiuser multiplexing provided by massive MIMO [1–5]. Despite the advantages offered by mmWave MIMO system, the need to deploy high-resolution analog-to-digital converters (ADCs) and digital-to-analog converters (DACs) for the large number of antenna elements in the base station (BS) makes system impractical in terms of the power consumption for the large arrays found in massive MIMO and the higher bandwidths in mmWave and sub-THz communications. The use of low-resolution (1-3 bits) ADCs/DACs is one approach to reduce overall transceiver power consumption [7, 9–12]. The most benefits in terms of power consumption and reduced analog hardware complexity are found with one-bit data converters, where the

conventional treatment of quantization error as additive noise may be a poor assumption.

Channel estimation is required for most one-bit receiver designs and has been widely considered in prior works [8, 11, 13–17]. Of relevance to our paper, in [13] and [14], the maximum-likelihood (ML) approach has been used to handle uplink (UL) channel estimation problem, but the prohibitive computational cost required for implementing the proposed algorithms has been the main impediment in practical scenarios. In [15], an algorithm referred to as Bussgang linear minimum mean squared error (BLMMSE) channel estimation has been developed for both flat and frequency-selective channel models. The essence of BLMMSE is to approximate the non-linear one-bit quantizer as a linear function via the Bussgang decomposition [18]. In [11], the authors have proposed a generalized approximate message passing (GAMP) based algorithm, where a compressive sensing (CS) approach has been employed to estimate the angular domain parameters of UL channel. In [16], an amplitude retrieval (AR) based algorithm has been derived that is based on completing the lost amplitudes of one-bit measurements along with ML direction-of-arrival (DOA) estimation method. Recently, an algorithm referred to as gridless GAMP (GL-GAMP) has been developed in [17] for UL channel estimation. GL-GAMP utilizes modified expectation-maximization GAMP (EM-GAMP) method in conjunction with the well-known RELAX [19] method to reconstruct the channel. Motivated by the promising use of the structure-based methods such as the AR and GL-GAMP methods, we develop a channel estimation approach by leveraging the underlying Toeplitz structure of the UL channel along with angular domain sparsity, which has not been fully exploited in prior works.

In this paper, we develop a new method referred to as sparsity enforcing with Toeplitz matrix reconstruction (SE-TMR) method to address the problem of UL channel estimation for mmWave MIMO communications when one-bit ADCs are deployed at the BS. The core idea of SE-TMR is to first reformulate UL channel estimation problem in terms of multiplication of two specific matrices, followed by using the combination of Toeplitz matrix reconstruction and UL channel sparsity in the angular domain. SE-TMR reconstructs efficiently UL channel up to a scale factor. Numerical simula-

This work was supported in part by Academy of Finland under Research Grant 319822.

tions validate its performance improvement and compare it to the existing competitive methods.

Notations: Upper-case and lower-case bold-face letters denote matrices and vectors, respectively, while scalars are denoted by lower-case letters. The transpose, and Hermitian transpose are denoted by $\{\cdot\}^T$ and $\{\cdot\}^H$, respectively, while $\|\cdot\|$ and $\|\cdot\|_1$ denote the l_2 and l_1 norms of a vector, and $\|\cdot\|_F$ stands for the Frobenius norm of a matrix. The notation $\mathcal{T}(\cdot)$ stands for an operation of building a square Hermitian Toeplitz matrix with its first column being the bracketed vector, and $\text{trace}\{\cdot\}$ stands for the trace of a square matrix. The $n \times n$ identity matrix is denoted by \mathbf{I}_n . The $n \times 1$ vector with all its entries equal to one is denoted by $\mathbf{1}_n$. The i th entry of the vector $\boldsymbol{\pi}$ is denoted by $[\boldsymbol{\pi}]_i$, while the entry in the intersection of the i th row and j th column of the matrix $\mathbf{\Pi}$ is denoted as $[\mathbf{\Pi}]_{i,j}$. The operator $\text{vec}\{\cdot\}$ stacks the columns of a matrix into a long vector. The operator $\text{diag}\{\boldsymbol{\pi}\}$ generates a diagonal matrix by plugging the entries of the vector $\boldsymbol{\pi}$ into its main diagonal. Finally, $\Re\{\cdot\}$ and $\Im\{\cdot\}$ return the real and imaginary parts of the bracketed argument, respectively.

2. UL CHANNEL ESTIMATION

2.1. System Model

Consider an UL multiuser mmWave MIMO system equipped with a uniform linear array (ULA) of M antenna elements at the base station (BS) and K single antenna users. The BS is equipped with one-bit ADCs, whereas all users deploy high-resolution DACs. Then, the UL channel between user k and the BS can be formulated as

$$\begin{aligned} \mathbf{h}_k &= \sum_{l=1}^{L_k} \sum_{m=1}^{M_{\text{path}}^{k,l}} \gamma_{k,l,m} \mathbf{a}(\theta_{k,l,m}) \\ &= [\mathbf{A}(\boldsymbol{\theta}_{k,1}), \dots, \mathbf{A}(\boldsymbol{\theta}_{k,L_k})] \begin{bmatrix} \gamma_{k,1} \\ \vdots \\ \gamma_{k,L_k} \end{bmatrix} = \mathbf{A}(\boldsymbol{\theta}_k) \boldsymbol{\gamma}_k \end{aligned} \quad (1)$$

where L_k denotes the number of multipath clusters between the BS and the user k , the l th cluster encompasses $M_{\text{path}}^{k,l}$ paths concentrated around an angular area defined by the corresponding angle spread [20], $\gamma_{k,l,m}$ and $\theta_{k,l,m}$ are respectively the gain and DOA of the m th path in the l th cluster, the steering vector is set as $\mathbf{a}(\theta_{k,l,m}) = [1, e^{-j\pi \sin(\theta_{k,l,m})}, \dots, e^{-j(M-1)\pi \sin(\theta_{k,l,m})}]^T \in \mathbb{C}^{M \times 1}$, $\boldsymbol{\theta}_{k,l} \triangleq [\theta_{k,l,1}, \dots, \theta_{k,l,M_{\text{path}}^{k,l}}]^T \in \mathbb{R}^{M_{\text{path}}^{k,l} \times 1}$ for $l = 1, \dots, L_k$, $\mathbf{A}(\boldsymbol{\theta}_{k,l}) \triangleq [\mathbf{a}(\theta_{k,l,1}), \dots, \mathbf{a}(\theta_{k,l,M_{\text{path}}^{k,l}})] \in \mathbb{C}^{M \times M_{\text{path}}^{k,l}}$, $\boldsymbol{\gamma}_{k,l} \triangleq [\gamma_{k,l,1}, \dots, \gamma_{k,l,M_{\text{path}}^{k,l}}]^T \in \mathbb{C}^{M_{\text{path}}^{k,l} \times 1}$, $\boldsymbol{\theta}_k \triangleq [\boldsymbol{\theta}_{k,1}^T, \dots, \boldsymbol{\theta}_{k,L_k}^T]^T$, $\mathbf{A}(\boldsymbol{\theta}_k) \triangleq [\mathbf{A}(\boldsymbol{\theta}_{k,1}), \dots, \mathbf{A}(\boldsymbol{\theta}_{k,L_k})]$, and $\boldsymbol{\gamma}_k \triangleq [\boldsymbol{\gamma}_{k,1}^T, \dots, \boldsymbol{\gamma}_{k,L_k}^T]^T$. The overall channel between the BS and K users is

$$\mathbf{H} = [\mathbf{h}_1, \dots, \mathbf{h}_K] = [\mathbf{A}(\boldsymbol{\theta}_1) \boldsymbol{\gamma}_1, \dots, \mathbf{A}(\boldsymbol{\theta}_K) \boldsymbol{\gamma}_K]. \quad (2)$$

In the training stage, a pilot sequence of length N_s ($N_s \geq K$) is transmitted by K users. The received signal at the BS is

$$\mathbf{Y} = \mathcal{Q}(\mathbf{H}\mathbf{S} + \mathbf{N}) \quad (3)$$

where $\mathcal{Q}(\cdot) \triangleq \text{sign}(\Re\{\cdot\}) + j\text{sign}(\Im\{\cdot\})$ is the element-wise one-bit quantizer which maps an argument to one of the members of the set $\mathcal{S} = \{1+j, 1-j, -1+j, -1-j\}$, $\mathbf{S} \in \mathbb{C}^{K \times N_s}$ represents the orthogonal pilot matrix, and $\mathbf{N} \in \mathbb{C}^{M \times N_s}$ is the additive circularly symmetric complex-valued Gaussian noise with zero mean and variance σ^2 . The aim is to recover (scaled) $\mathbf{H} \in \mathbb{C}^{M \times K}$ by processing the received signal $\mathbf{Y} \in \mathbb{C}^{M \times N_s}$.

2.2. Proposed UL Channel Estimation

Our UL channel estimation method will be developed by employing the notion of Toeplitz matrix reconstruction combined with the angular domain sparsity of UL channel. Although the actual channel between the BS and the k th user presented in (1) is composed of many paths, it is still sparse in an angular-based dictionary (e.g., the normalized discrete Fourier transform (DFT) matrix). Therefore, \mathbf{h}_k can be approximated as an unknown linear combination of a few atoms of the angular-based dictionary which correspond to those paths that contribute the most. These paths are entitled as the “*basis paths*” henceforth. From this point of view, we represent the k th column of \mathbf{H} (i.e., \mathbf{h}_k) as a linear combination of L_k basis paths with L_k path gains and DOAs. As a result, (2) can be recast as

$$\mathbf{H} = [\mathbf{h}_1, \dots, \mathbf{h}_K] = [\mathbf{A}(\bar{\boldsymbol{\theta}}_1) \bar{\boldsymbol{\gamma}}_1, \dots, \mathbf{A}(\bar{\boldsymbol{\theta}}_K) \bar{\boldsymbol{\gamma}}_K] \quad (4)$$

where $\bar{\boldsymbol{\theta}}_k \triangleq [\bar{\theta}_{k,1}, \dots, \bar{\theta}_{k,L_k}]^T \in \mathbb{R}^{L_k \times 1}$ and $\bar{\boldsymbol{\gamma}}_k \triangleq [\bar{\gamma}_{k,1}, \dots, \bar{\gamma}_{k,L_k}]^T \in \mathbb{C}^{L_k \times 1}$ are respectively the DOAs and path gains which correspond to L_k basis paths between the BS and user k .

To develop our method, we first reformulate (4) as

$$\mathbf{H} = \mathbf{A} \boldsymbol{\Gamma} \bar{\mathbf{G}} = \bar{\mathbf{H}} \bar{\mathbf{G}} \quad (5)$$

where

$$\mathbf{A} \triangleq [\mathbf{A}(\bar{\boldsymbol{\theta}}_1), \dots, \mathbf{A}(\bar{\boldsymbol{\theta}}_K)] \in \mathbb{C}^{M \times L} \quad (6)$$

$$\boldsymbol{\Gamma} \triangleq \begin{bmatrix} \text{diag}(\bar{\boldsymbol{\gamma}}_1) & & & \\ & \ddots & & \\ & & \text{diag}(\bar{\boldsymbol{\gamma}}_K) & \\ & & & \end{bmatrix} \in \mathbb{C}^{L \times L} \quad (7)$$

$$\bar{\mathbf{G}} \triangleq \begin{bmatrix} \mathbf{1}_{L_1} & & & \\ & \mathbf{1}_{L_2} & & \\ & & \ddots & \\ & & & \mathbf{1}_{L_K} \end{bmatrix} \in \mathbb{R}^{L \times K} \quad (8)$$

$$\bar{\mathbf{H}} \triangleq \mathbf{A} \boldsymbol{\Gamma} \in \mathbb{C}^{M \times L} \quad (9)$$

and $L \triangleq \sum_{k=1}^K L_k$. The significant point stated in (5) is that estimating \mathbf{H} is equivalent to estimating $\bar{\mathbf{H}}$. Therefore, we develop SE-TMR by formulating an optimization problem with respect to $\bar{\mathbf{H}}$ because of good properties that $\bar{\mathbf{H}}$ possesses as it will be elaborated in the sequel.

Due to the special structures of \mathbf{A} and $\mathbf{\Gamma}$, i.e., \mathbf{A} and $\mathbf{\Gamma}$ being respectively Vandermonde and diagonal matrices, it is straightforward to show that

$$\bar{\mathbf{H}}\bar{\mathbf{H}}^H = \mathcal{T}(\mathbf{u}) \quad (10)$$

where $\mathbf{u} \in \mathbb{C}^M$ and $[\mathbf{u}]_1$ belongs to the real numbers field.

Moreover, the channel estimation problem can be converted into a sparse recovery problem by defining an angular-based dictionary [21, 22] as explained above. In the case of ULA, the normalized DFT matrix can be a proper dictionary [17] because of zero intra-column correlation, i.e., the DFT matrix columns are orthonormal to each other. Hence, multiplying $\bar{\mathbf{H}}$ by the DFT matrix, we have

$$\mathbf{X}(\bar{\boldsymbol{\theta}}) = \mathbf{F}\bar{\mathbf{H}} = \mathbf{F}\bar{\mathbf{H}}\bar{\mathbf{G}} \quad (11)$$

where $\mathbf{F} \in \mathbb{C}^{M \times M}$ denotes the normalized DFT matrix. Taking into consideration (5), it can be concluded that each column of $\mathbf{X}(\bar{\boldsymbol{\theta}})$ defined in (11) is sparse. It is well known that the optimal way to enforce sparsity is to use l_0 pseudo-norm, however, the corresponding optimization problem is known to be NP hard. Therefore, we exploit l_1 norm to enforce sparsity, which is a widely used alternative.

Considering (10) and (11), the following optimization problem is introduced to recover $\bar{\mathbf{H}}$ efficiently given the one-bit measurement matrix \mathbf{Y}

$$\min_{\bar{\mathbf{H}}, \mathbf{u}, \mathbf{E}^R, \mathbf{E}^I} \|\text{vec}\{\mathbf{F}\bar{\mathbf{H}}\bar{\mathbf{G}}\}\|_1 + \lambda \left(\sum_{i=1}^M \sum_{j=1}^{N_s} ([\mathbf{E}^R]_{i,j} + [\mathbf{E}^I]_{i,j}) \right) \quad (12)$$

$$\text{s.t.} \quad \bar{\mathbf{H}}\bar{\mathbf{H}}^H = \mathcal{T}(\mathbf{u}) \quad (13)$$

$$\text{trace}\{\mathcal{T}(\mathbf{u})\} = C \quad (14)$$

$$\Re\{[\bar{\mathbf{H}}\bar{\mathbf{G}}\mathbf{S}]_{i,j}\} \Re\{[\mathbf{Y}]_{i,j}\} \geq -[\mathbf{E}^R]_{i,j}, \quad i = 1, \dots, M, \quad j = 1, \dots, N_s \quad (15)$$

$$\Im\{[\bar{\mathbf{H}}\bar{\mathbf{G}}\mathbf{S}]_{i,j}\} \Im\{[\mathbf{Y}]_{i,j}\} \geq -[\mathbf{E}^I]_{i,j}, \quad i = 1, \dots, M, \quad j = 1, \dots, N_s \quad (16)$$

$$[\mathbf{E}^R]_{i,j} \geq 0, \quad i = 1, \dots, M, \quad j = 1, \dots, N_s \quad (17)$$

$$[\mathbf{E}^I]_{i,j} \geq 0, \quad i = 1, \dots, M, \quad j = 1, \dots, N_s \quad (18)$$

where $\lambda > 0$ is a regularization parameter, the entries of $\mathbf{E}^R \in \mathbb{R}^{M \times N_s}$ and $\mathbf{E}^I \in \mathbb{R}^{M \times N_s}$ are slack variables introduced to handle probable sign flips due to the impact of noise [23]. In this problem, (14) prevents the scaling ambiguity with $C > 0$, and (15)–(16) are imposed to maintain the consistency with the observation matrix \mathbf{Y} . The optimization problem (12)–(18) is non-convex because of the constraint

(13) which is difficult to address in an efficient manner. For alleviating difficulties caused by imposing (13), semi-definite programming (SDP) relaxation can be exploited to turn the non-convex constraint (13) into a convex one. Therefore, the optimization problem (12)–(18) can be modified by means of SDP relaxation as

$$\min_{\bar{\mathbf{H}}, \mathbf{u}, \mathbf{E}^R, \mathbf{E}^I} \|\text{vec}\{\mathbf{F}\bar{\mathbf{H}}\bar{\mathbf{G}}\}\|_1 + \lambda \left(\sum_{i=1}^M \sum_{j=1}^{N_s} ([\mathbf{E}^R]_{i,j} + [\mathbf{E}^I]_{i,j}) \right) \quad (19)$$

$$\text{s.t.} \quad \begin{bmatrix} \mathbf{I}_L & \bar{\mathbf{H}}^H \\ \bar{\mathbf{H}} & \mathcal{T}(\mathbf{u}) \end{bmatrix} \succeq 0 \quad (20)$$

$$[\mathbf{u}]_1 = \frac{C}{M} \quad (21)$$

$$\Re\{[\bar{\mathbf{H}}\bar{\mathbf{G}}\mathbf{S}]_{i,j}\} \Re\{[\mathbf{Y}]_{i,j}\} \geq -[\mathbf{E}^R]_{i,j}, \quad i = 1, \dots, M, \quad j = 1, \dots, N_s \quad (22)$$

$$\Im\{[\bar{\mathbf{H}}\bar{\mathbf{G}}\mathbf{S}]_{i,j}\} \Im\{[\mathbf{Y}]_{i,j}\} \geq -[\mathbf{E}^I]_{i,j}, \quad i = 1, \dots, M, \quad j = 1, \dots, N_s \quad (23)$$

$$[\mathbf{E}^R]_{i,j} \geq 0, \quad i = 1, \dots, M, \quad j = 1, \dots, N_s \quad (24)$$

$$[\mathbf{E}^I]_{i,j} \geq 0, \quad i = 1, \dots, M, \quad j = 1, \dots, N_s \quad (25)$$

where the convex constraint (20) is imposed instead of (13) via SDP relaxation, and (14) is replaced by (21) as they are interchangeable. The optimization problem (19)–(25) is convex and therefore can be solved by off-the-shelf solvers like CVX [24].

After estimating $\bar{\mathbf{H}}$, we recover \mathbf{H} using (5). Due to the angular-based structure of the columns of $\bar{\mathbf{H}}$, further refinement can be attained through recovering the L_k^{HR} path gains and L_k^{HR} DOAs associated with the k th column of $\bar{\mathbf{H}}$ for $k = 1, \dots, K$. In doing so, conventional one-dimensional harmonic retrieval (HR) methods such as RELAX [19] can be applied to each column of $\bar{\mathbf{H}}$ in order to estimate the L_k^{HR} path gains and L_k^{HR} DOAs, and then reconstruct the refined \mathbf{H} [17], denoted by $\hat{\mathbf{H}}$. Note that L_k^{HR} can be opted greater than L_k due to the presence of actual larger number of multipaths than the basis paths as given in (1). As a matter of fact, it will be shown in the next section by means of simulation that choosing L_k^{HR} greater than L_k leads to performance improvement of the SE-TMR method. The steps of the proposed UL channel estimator are outlined in Algorithm 1.

3. SIMULATION RESULTS

We evaluate the performance of the proposed SE-TMR method and compare it to that of other competitive algorithms. The methods used for comparison are near ML (nML) [13], AR [16], and zero-forcing (ZF) method of [13]. A Zadoff-Chu (ZC) sequence with length N_s is used to construct the pilot sequence, such that each row of \mathbf{S} is a circularly shifted replica of the ZC sequence and is therefore

Algorithm 1: SE-TMR Algorithm

Input: \mathbf{Y} , $\bar{\mathbf{G}}$, λ , L_k 's, L_k^{HR} 's

1: Obtain $\bar{\mathbf{H}}$, \mathbf{u} , \mathbf{E}^R , and \mathbf{E}^I by solving the optimization problem (19)-(25).

2: Calculate $\mathbf{H} = \bar{\mathbf{H}}\bar{\mathbf{G}}$.

Refinement with RELAX:

3: Apply RELAX to each column of \mathbf{H} to estimate each user's L_k^{HR} DOAs and path gains.

4: Employ the estimated DOAs and path gains of each user to recover the channel matrix $\hat{\mathbf{H}}$.

Output: $\hat{\mathbf{H}}$

orthogonal to the other rows.¹ The signal-to-noise ratio (SNR) and normalized mean square error (NMSE) are respectively defined as $\text{SNR} \triangleq 10 \log_{10} \left(\frac{\|\mathbf{S}\|_F^2}{N_s \sigma^2} \right)$ and $\text{NMSE} \triangleq$

$$\frac{1}{KN} \sum_{k=1}^K \sum_{n=1}^N \left\| \frac{\hat{\mathbf{h}}_k^{(n)}}{\|\hat{\mathbf{h}}_k^{(n)}\|} - \frac{\mathbf{h}_k}{\|\mathbf{h}_k\|} \right\|^2,$$

where $\hat{\mathbf{h}}_k^{(n)}$ is the k th column of $\hat{\mathbf{H}}$ estimated in the n th Monte Carlo run, and N is the total number of Monte Carlo runs which is $N = 100$ in this paper. We consider $\lambda = 10$, and $K = 8$ in all examples.² Moreover, the same number of channel clusters and within cluster multipaths for each user are considered in the upcoming examples,³ i.e., $L_1 = \dots = L_K$ and $M_{\text{path}}^{1,1} = \dots = M_{\text{path}}^{1,L_1} = \dots = M_{\text{path}}^{K,1} = \dots = M_{\text{path}}^{1,L_K} = 100$. All UL DOAs are generated randomly once and remain the same throughout the Monte Carlo runs. Moreover, the channel path gains are distributed as $\mathcal{CN}(0, 1)$ for all users. Fig. 1 shows the NMSE performance of the methods tested versus SNR for the setup of $M = 16$, $N_s = 128$, and $L_k = 1$. Moreover, the angle spread within a cluster is 8 degrees. Note that L_k^{HR} is set as 4 for the SE-TMR method in this example. It shows that the performance of the proposed SE-TMR method is substantially better than that of the other methods tested. Note that RELAX method is also applied to nML and ZF methods (see steps 3 and 4 in Algorithm 1) to reconstruct the structured estimate of the UL channel. Hence, the original methods without RELAX-based refinement are called “unstructured” in the figures.⁴ The setup considered for Fig. 2 is $M = 16$, $N_s = 128$, and $L_k = 2$. The angle spread within one cluster is 8 degrees, while it is 10 degrees for the other one. In Fig. 2, the proposed SE-TMR method outperforms the other

¹In our algorithm, the choice of pilot sequence is not of significance, i.e., our algorithm also works with other pilot sequences. ZC sequence is selected here solely due to its popularity.

²It is observed that setting λ much greater than one leads to better performance, i.e., $\lambda \gg 1$.

³Different users may have different numbers of channel clusters and multipaths within clusters. For simplicity, we use the same number of channel clusters and within cluster multipaths for all users here.

⁴RELAX method is not applied to AR since the AR algorithm uses an ML DOA estimator as one step of the channel estimation algorithm, therefore, it belongs to the category of structured methods.

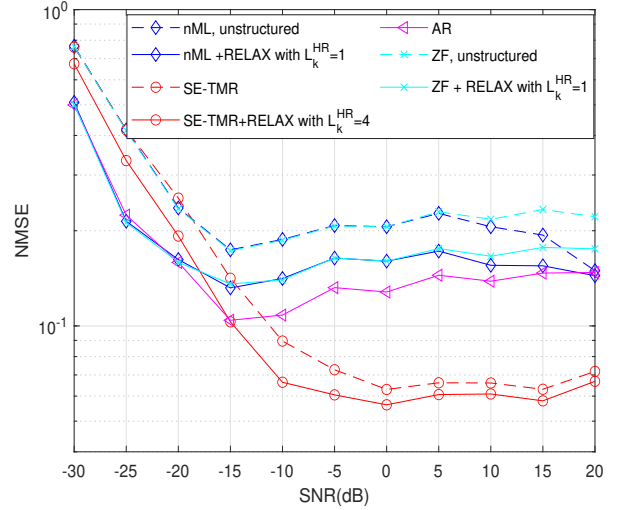


Fig. 1. NMSE vs. SNR for $M = 16$, $N_s = 128$, and $L_k = 1$.

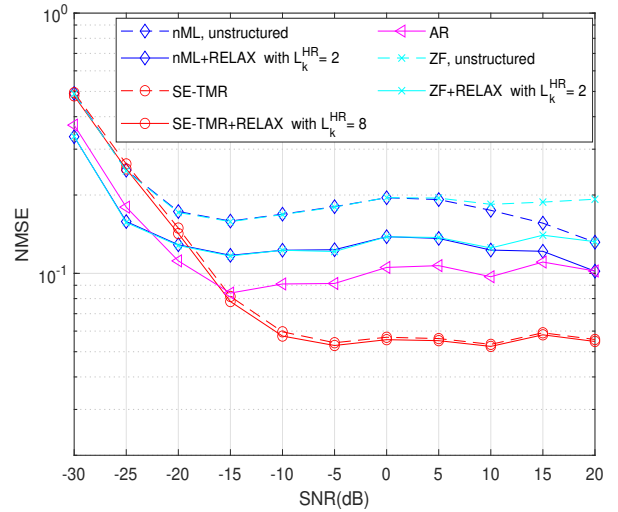


Fig. 2. NMSE vs. SNR for $M = 16$, $N_s = 128$, and $L_k = 2$.

methods tested.

4. CONCLUSION

A novel algorithm called SE-TMR is presented to estimate UL channel in mmWave multi-user MIMO systems with one-bit ADCs at the BS. The essence of the SE-TMR method is to reconstruct UL channel by solving a properly designed optimization problem, which leverages the Toeplitz matrix reconstruction and sparsity of UL channel in the DFT domain. Based on the numerical simulations provided, the SE-TMR method outperforms existing competitive methods in different scenarios with diverse number of dominated paths between the BS and users.

5. REFERENCES

- [1] E. G. Larsson, O. Edfors, F. Tufvesson, and T. L. Marzetta, "Massive MIMO for next generation wireless systems," *IEEE Commun. Mag.*, vol. 52, no. 2, pp. 186–195, Feb. 2014.
- [2] F. Boccardi, R. W. Heath, A. Lozano, T. L. Marzetta, and P. Popovski, "Millimeter-wave massive MIMO: The next wireless revolution?," *IEEE Commun. Mag.*, vol. 52, no. 2, pp. 74–80, Feb. 2014.
- [3] A. L. Swindlehurst, E. Ayanoglu, P. Heydari, and F. Capolio, "Five disruptive technology directions for 5G," *IEEE Comm. Mag.*, vol. 52, no. 9, pp. 56–62, Sep. 2014.
- [4] R. W. Heath, N. Gonzalez-Prelcic, S. Rangan, W. Roth, and A. M. Sayeed, "An overview of signal processing techniques for millimeter wave MIMO systems," *IEEE J. Sel. Top. Signal Process.*, vol. 10, no. 3, pp. 436–453, Apr. 2016.
- [5] T. S. Rappaport *et al.*, "Millimeter Wave Mobile Communications for 5G Cellular: It Will Work!," *IEEE Access*, vol. 1, pp. 335–349, May. 2013.
- [6] R. H. Walden, "Analog-to-digital converter survey and analysis," *IEEE J. Sel. Areas Commun.*, vol. 17, no. 4, pp. 539–550, Apr. 1999.
- [7] A. Mezghani, F. Antreich, and J. A. Nossek, "Multiple parameter estimation with quantized channel output," in *Proc. Int. ITG Workshop Smart Antennas*, Bremen, Germany, Feb. 2010, pp. 143–150.
- [8] C. Mollen, J. Choi, E. G. Larsson, and R. W. Heath Jr., "Uplink Performance of Wideband Massive MIMO With One-Bit ADCs," *IEEE Trans. Wireless Commun.*, vol. 16, no. 1, pp. 87–100, Jan. 2017.
- [9] C. Wen, C. Wang, S. Jin, K. Wong, and P. Ting, "Bayes-optimal joint channel-and-data estimation for massive MIMO with low-precision ADCs," *IEEE Trans. Signal Process.*, vol. 64, no. 10, pp. 2541–2556, May 2016.
- [10] S. Jacobsson, G. Durisi, M. Coldrey, U. Gustavsson, and C. Studer, "Throughput analysis of massive MIMO uplink with low-resolution ADCs," *IEEE Trans. Wireless Commun.*, vol. 16, no. 6, pp. 4038–4051, Jun. 2017.
- [11] J. Mo, P. Schniter, and R. W. Heath, "Channel estimation in broadband millimeter wave MIMO systems with few-bit ADCs," *IEEE Trans. Signal Process.*, vol. 66, no. 5, pp. 1141–1154, Mar. 2018.
- [12] J. Zhang, L. Dai, X. Li, Y. Liu, and L. Hanzo, "On low-resolution ADCs in practical 5G millimeter-wave massive MIMO systems," *IEEE Commun. Mag.*, vol. 56, no. 7, pp. 205–211, Jul. 2018.
- [13] J. Choi, J. Mo, and R. W. Heath, "Near maximum-likelihood detector and channel estimator for for uplink multiuser massive MIMO systems with one-bit ADCs," *IEEE Trans. Commun.*, vol. 64, no. 5, pp. 2005–2018, May 2016.
- [14] F. Wang, J. Fang, H. Li, Z. Chen, and S. Li, "One-bit quantization design and channel estimation for massive MIMO systems," *IEEE Trans. Veh. Technol.*, vol. 67, no. 11, pp. 10921–10934, Nov. 2018.
- [15] Y. Li, C. Tao, G. Seco-Granados, A. Mezghani, A. L. Swindlehurst, and L. Liu, "Channel estimation and performance analysis of one-bit massive MIMO systems," *IEEE Trans. Signal Process.*, vol. 65, no. 15, pp. 4075–4089, Aug. 2017.
- [16] C. Qian, X. Fu, and N. D. Sidiropoulos, "Amplitude retrieval for channel estimation of MIMO systems with one-bit ADCs," *IEEE Signal Process. Lett.*, vol. 26, no. 11, pp. 1698–1702, Nov. 2019.
- [17] L. Xu, C. Qian, F. Gao, W. Zhang, and S. Ma, "Angular domain channel estimation for mmWave massive MIMO with one-bit ADCs/DACs," *IEEE Trans. Wireless Commun.*, vol. 20, no. 2, pp. 969–982, Feb. 2021.
- [18] J. J. Bussgang, "Crosscorrelation functions of amplitude-distorted Gaussian signals," Res. Lab. Electron., Massachusetts Inst. Technol., Cambridge, MA, USA, Tech. Rep. 216, 1952.
- [19] J. Li and P. Stoica, "Efficient mixed-spectrum estimation with applications to target feature extraction," *IEEE Trans. Signal Process.*, vol. 44, no. 2, pp. 281–295, Feb. 1996.
- [20] "5G channel model for bands up to 100 GHz (v2.3)," Tech. Rep., 2016. [Online]. Available: <http://www.5gworkshops.com/5gcm.html>
- [21] W. U. Bajwa, J. Haupt, A. M. Sayeed, and R. Nowak, "Compressed channel sensing: A new approach to estimating sparse multipath channels," *Proc. IEEE*, vol. 98, no. 6, pp. 1058–1076, Jun. 2010.
- [22] B. Wang, F. Gao, S. Jin, H. Lin, and G. Y. Li, "Spatial-and-frequency-wideband effects in millimeter-wave massive MIMO systems," *IEEE Trans. Signal Process.*, vol. 66, no. 13, pp. 3393–3406, Jul. 2018.
- [23] Y. Gao, D. Hu, Y. Chen, and Y. Ma, "Gridless 1-b DOA estimation exploiting SVM approach," *IEEE Commun. Lett.*, vol. 21, no. 10, pp. 2210–2213, Oct. 2017.
- [24] M. Grant, S. Boyd, and Y. Ye, CVX: Matlab software for disciplined convex programming. 2008 [Online]. Available: <http://stanford.edu/~boyd/cvx>